Sedimentary environmental quality of a biosphere reserve estuary from Southwestern Iberian Peninsula

A. Barba-Lobo[1, 2, *], B. García-González[1], J.L. Guerrero[1,3], and J.P. Bolívar[1]

[1] Radiation Physics and Environment Group (FRYMA), Department of Integrated Sciences, Center for Natural Resources, Health and Environment (RENSMA), University of Huelva, 21007, Huelva, Spain

[2] Department of Medical Radiation Sciences, Institute of Clinical Sciences, Sahlgrenska Academy at University of Gothenburg, Gothenburg, SE-413 45, Sweden

[3]Department of Biology and Geology, Physics and Inorganic Chemistry, Higher School of Experimental Sciences and Technology, Rey Juan Carlos University, c/Tulipán s/n, 28933 Móstoles, Spain

ABSTRACT

The Huelva estuary is formed by the common mouths of the Odiel and Tinto Rivers, and inside this ecosystem is the biosphere reserve of the Odiel saltmarshes. This ecosystem has been historically affected by acid mine drainage (AMD) and by releases of pollutants from five phosphoric acid industrial plants and phosphogypsum (PG) waste stacks located in the area. Therefore, this study aims to carry out a comprehensive assessment of the environmental impact of the biosphere reserve of the Odiel saltmarshes. For this, it was necessary to find a suitable sedimentary background (Piedras River in our case). To quantify this impact, several pollution indexes were used. According to the values reached by the indexes, this impact was classified as "serious" pollution for most trace elements, excepting the deepest layers, and "low-moderate" pollution for the ^{238}U-series radionuclides, while no pollution for the ^{232}Th-series and ^{40}K radionuclides was found as expected.

Keywords: Phosphogypsum piles; Fertilizer industry; Acid mine drainage; Trace elements; Natural radionuclides; Pollution indexes

*Corresponding author.
E-mail address: alejandro.barba@dci.uhu.es, alejandro.barba-lobo@gu.se (A. Barba-Lobo)

1. Introduction

The estuary of Huelva is in the Southwestern Spain, and it is formed by the common mouths of the Tinto and Odiel Rivers (see Fig. 1), which are ones of the most polluted rivers in the world by acid mine drainage (AMD). Their waters contain very high levels of concentrations (3-5 orders of magnitude higher than unperturbed surface waters) of heavy metals and natural radionuclides, especially for U and Th isotopes (Guerrero et al., 2021a; Olías et al., 2006; Nieto et al., 2013; Nieto et al., 2007). In addition, in this estuary a very large industrial chemical complex is also located, whose activity began in 1965, including plants devoted to the production of fertilizers, ammonia, copper by smelting/electrorefining, oil refining, petrochemical, TiO_2 pigments, etc. Both pollution sources have produced a high historical pollution of this estuary from the XIX century to the present day (Borrego et al., 2002; Morillo et al., 2004; Pérez-López et al., 2011).

A big fraction of the basins of these rivers is in the Iberian pyrite belt (IPB), southwest of the Iberian Peninsula, one of the major deposits of massive polymetallic sulphurs in the world, being estimated a polymetallic sulphur reserve of about 1.7 Gt (Sáez et al., 1999). These deposits were mined by other civilizations such as Tartessos and Roman, but the greatest mining activity started in the second half of XIX century, mainly by British and French mining companies, generating in the North of the Huelva province old mining galleries, millings, and several types of waste (Mujica et al., 2008). These "legacy sites" contain the sources of the AMD problem in both Odiel and Tinto Rivers waters because the basins of these rivers receive waters from the IPB.

AMD is produced by the oxidation of these residual materials that interact with the water and its dissolved oxygen, generating the release of Fe^{2+} and a great acidification of the aqueous medium reaching pH up to 1-2 (Aduvire, 2006). These sulphurs are mainly composed by iron pyrite (FeS_2), and variable proportions of other subordinate minerals as sphalerite (ZnS), galena (PbS), chalcopyrite ($CuFeS_2$), arsenopyrite (FeAsS), pyrrhotite ($Fe_{1-x}S$), and many other minor phases, such as Bi- and Pb-sulfosalts, cassiterite, magnetite, stannite, electrum and cobaltite. The AMD process makes those minor elements contained in the sulphur minerals and their host-rocks to be released into the aqueous matrix (heavy metals, rare earth elements, radionuclides, etc.), generating very polluted waters (Curcio et al., 2019).

Another pollution problem in the Huelva estuary is related to the chemical industrial complex located in its vicinity, whose plants have released huge amounts of pollutants, mainly heavy metals, natural radionuclides, and anions into the Huelva estuary. In relation to the phosphoric acid production, 5 production plants were installed in the estuarine zone, using phosphate rock (PR) from Morocco as main raw material. The Moroccan phosphate rock is characterized by having a high concentration of ^{238}U (around 1500 Bq kg^{-1}, equivalent to about 50 ppm of natural U), which is about 50 times higher than the concentration of ^{238}U for a non-polluted soil (UNSCEAR, 2000). During the process, a by-product called phosphogypsum (PG) is generated, containing more than 95% of the majority of radioactivity initially contained in the raw material (^{226}Ra, ^{230}Th and ^{210}Pb), but only about 10-20% of ^{238}U (Bolívar et al., 2009; Gázquez et al., 2009).

Three different periods are distinguished in the PG management. The first one goes from 1965 to 1997, when the 20% of the PG was discharged directly into the Odiel channel and the remaining 80% was transported by using estuarine water, and finally deposited in piles in the right shore of the Tinto River channel, while the water used in the transport, with a pH around 1.5 and high concentration of metals and radionuclides, was returned into the Tinto River (Bolívar et al., 2008; Bolívar et al., 1995; García-Tenorio and García-León, 1996; Gázquez et al., 2009). During the second period (1998 to the end of 2010), the full PG generated in the 5 plants of phosphoric acid was pumped by using freshwater in a closed circuit since the used water was pumped back into the factories to be employed newly for PG pumping. And finally, on December 31st, 2010, the PA production was stopped, and since this date there has been no generation of phosphogypsum in Huelva (Hierro et al., 2012).

The main problem related to the PG direct discharges into the Odiel channel, and to a lesser extent the leachates from PG waste piles, are the releases of a great number of natural radionuclides such as ^{238}U, ^{226}Ra, ^{210}Pb or ^{210}Po, and toxic elements like Fe, Zn, As, Cr or Cd to their surroundings (Papaslioti et al., 2018; Pérez-López et al., 2016; Guerrero et al., 2021a,b)). Nowadays there are around 100 Mt of phosphogypsum distributed along 1000 ha on the occidental shore of the Tinto River, divided into 4 different areas (Hierro et al., 2013).

For these reasons, that is, due to both AMD releases and phosphogypsum leachates (PGL), the estuary of Huelva has a significant pollution level, which is caused by releases of trace elements and natural radionuclides. This can be corroborated by other studies on the pollution in the Odiel and Tinto Rivers (Borrego et al., 2002; Pérez-López et al., 2011).

Consequently, the aim of this study is to assess and update the environmental impact on the Odiel River estuarine biosphere reserve and for that, vertical profiles were analyzed. Furthermore, different pollution indexes were obtained in order to assess the environmental impact, which was possible due to the proper selection of a sedimentary background, also called baseline, that needs to be geochemically similar to the problem sedimentary system (Le Gall et al., 2018; Luo et al., 2022).

Considering everything previously mentioned, to the best of our knowledge, this is the most updated study on the environmental impact of the estuarine biosphere reserve from the Southwestern Iberian Peninsula. In addition, an exhaustive assessment and establishment of a proper sedimentary background (Piedras River in our case) was carried out, and the comparison with several sedimentary backgrounds placed at the Southwestern Iberian Peninsula was made. Moreover, the quantification of the impact in Bacuta Island was carefully accomplished using several pollution and toxicity indexes for major and trace elements, heavy metals and natural radionuclides, where the different pollution sources were identified by using correlation analysis. Furthermore, the procedure followed in this study to select a suitable sedimentary background, assess the environmental impact in the sedimentary system of interest and identify the different pollution sources can be applied to any sedimentary system worldwide, which makes this study be even more applicable.

2. Materials and methods

2.1 Sampling

Samplings were carried out in November 2021, taking a sediment core from Bacuta Island in the biosphere reserve of the Odiel saltmarshes and another one from the Piedras River, using this latter as sedimentary reference system to assess the background of this geographical area. This was necessary because it must have similar geochemical substrate that Huelva estuary, and do not contain a detectable influence from AMD or PG stacks and chemical complex (see Fig. 1). Every core had about 60 cm of depth and was cut into 2 cm thick sections (Fig. A.1, in Supplementary Material – Appendix A). Then, the 2 cm thick samples were dried in an oven at 60 ºC until constant weight, grinded by using an agate mortar, and finally well homogenized.

Fig. 1. Study area selected for the samplings carried out in this work, which the sediment cores were taken from Piedras River and Bacuta Island.

2.2 Characterization techniques

The major elements were analyzed by X-ray fluorescence (XRF) using the instrument Panalytical Spectrometer AXIOS at the Research, Technology and Innovation Centre of the University of Seville (CITIUS). Trace elements were analysed by inductively coupled plasma mass spectrometry (ICP-MS) at Activation Laboratories (Actlabs, Ontario, Canada), for which the samples were previously digested with strong acids such as hydrofluoric acid, followed by a mixture of nitric and perchloric acids. Granulometric analysis was carried out by laser diffraction, using the equipment Malvern Mastersizer 2000 by the General Services of the University of Huelva. The radionuclides by gamma-ray spectrometry were determined by using a well-type high purity germanium (HPGe) detector and an extended range HPGe detector (XtRa), whose efficiency calibrations were developed by Barba-Lobo et al. (2021a) and Barba-Lobo et al.

(2021b), respectively. This technique is widely used by the Radiation Physics and Environment Research Group (FRYMA) of the University of Huelva.

2.3 Quality control

All the measurements that were not carried out by the research group FRYMA, were ordered to accredited external laboratories. For every measurement, one replica and one blank per each ten samples were included, as well as certificated reference materials (CRMs) provided by the IAEA (International Atomic Energy Agency), where two CRMs were of soil type (IAEA-326 and IAEA-327) and another of phosphogypsum type (IAEA-434), obtaining generally z_{score} values less than 2. In addition, the laboratory of the group FRYMA annually participates in several intercomparison exercises, where gamma-ray spectrometry was employed for the analysis. To guarantee the reliability of the results, many different comparisons between different analysis techniques were accomplished such as the comparison between ICP-MS and gamma-ray spectrometry. Regarding the detection limits obtained for ICP-MS and gamma-ray spectrometry, they were ranged from 0.05 ppm and 0.1 ppm, and from 2 Bq kg^{-1} to 20 Bq kg^{-1}, respectively.

In addition, the validation for gamma-ray spectrometry was also accomplished by comparing the ^{40}K concentration obtained by using gamma-ray spectrometry with that concentration obtained by means of XRF using the relationship: 1% of natural K → 313 mBq/g of ^{40}K (Barba-Lobo et al., 2021a).

2.4 Pollution and toxicity indexes

To evaluate the environmental impact in the Huelva estuarine by AMD and phosphogypsum discharges, several pollution indexes have been used and the classification for every pollution index is shown in Table A.1 (Supplementary Material – Appendix A).

2.4.1 Enrichment factor (EF)

The enrichment factor for an element (i) in a sample (s), EF_i, has been used to evaluate the degree of anthropic pollution in soils and sediments by using a conservative element as normalizer of the concentrations, being Al the most one used (Díaz-Asencio et al., 2011; Hakason, 1979; Lario et al., 2016; Zhang et al., 2016). The *EF* can be calculated by Eq. 1:

$$EF_i = \frac{\left({C_i}/{C_{Al}}\right)_s}{\left({C_i}/{C_{Al}}\right)_r} \quad (1)$$

where C_i is the concentration of a specific element (i) in the sample (s), $(C_i)_s$, and in the reference (r), $(C_i)_r$, and C_{Al} is the concentration of Al in the sample, $(C_{Al})_s$, and in the reference, $(C_{Al})_r$.

2.4.2 Contamination factor (CF)

To estimate the pollution level about a specific element with respect a typical soil, the contamination factor, *CF*, is calculated using the following equation (Gözel et al., 2022; Vineethkumar et al., 2020):

$$CF_i = \frac{(C_i)_s}{(C_i)_r} \quad (2)$$

where $(C_i)_s$ is the concentration of an element (i) present in the sample (s) and $(C_i)_r$ is referred to the concentration of this element reference (r) system, which in our case was taken from (Rudnick and Gao, 2003).

For the *CF* assessment in the case of natural radionuclides, that is, ^{238}U-series, ^{232}Th-series and ^{40}K, the activity concentrations stablished by UNSCEAR (2000) for unpolluted typical soils, that is, 35 Bq kg^{-1}, 30 Bq kg^{-1} and 400 Bq kg^{-1} for ^{238}U, ^{232}Th and ^{40}K, respectively, were used as reference activity concentrations.

2.4.3 Contamination degree (CD)

The contamination degree (*CD*) is a factor to measure the mean level of contamination of a sample/material by considering all the toxic elements, such as As, Cd, Cr, Cu, Ni, Pb and Zn, and can be calculated by the following equation (Vineethkumar et al., 2020; Yushin et al., 2023):

$$CD = \frac{\sum_{i=1}^{n} FC_i}{n} \quad (3)$$

where *n* is the number of elements (i) considered for the CD calculation.

2.4.4 Potential ecological risk (PER)

The potential ecological risk (*PER*) is a factor by which it is possible to assess the toxicity associated with the presence of heavy metals (Kerolli-Mustafa et al., 2015; Liu et al., 2021), that is, Cd, Cr, Cu, Ni, Pb and Zn, as well as As (metalloid) (a total of seven elements). The *PER* for an element "i" is calculated by the following equation:

$$PER_i = CF_i \cdot T_i \quad (4)$$

where CF_i is the contamination factor of the element (i), and T_i is the toxicity factor for this element, that is, T_i is based on the principle of abundance, which indicates that the potential toxicological effect of an element is proportional to its abundance, or rarity, in nature. The T_i has a specific value for each heavy metal and As (Kerolli-Mustafa et al., 2015; Liu et al., 2021).

2.4.5 Potential toxicity of a sample (PT)

Regarding the potential risk that a sample or material can produce, potential toxicity index (*PT*) is defined, and it is calculated as follows (Kerolli-Mustafa et al., 2015):

$$PT = \sum_i PER_i \quad (5)$$

2.5 Data treatment

In the case of the data treatment, a principal component analysis (PCA) was performed providing the data interpretation by using the XLSTAT software (Lumivero, 2023). Firstly, the calculation of the correlation matrix of the variables was carried out, starting from the matrix of original data. Then, the calculation of the factor matrix, starting from the Pearson's "r" of the previous matrix.

3. Results and discussion

For the cores taken from the Piedras River and Bacuta Island, firstly a granulometric analysis was done to evaluate the pollutants sorption capacity of the samples, and then, concentrations of stable elements (major and trace elements) were measured. Afterwards, the suitability of the Piedras River as a sedimentary background was tested, and the environmental impact in Bacuta Island was assessed. Finally, correlation analysis was carried out for Piedras River and Bacuta Island in order to find the influence of the pollution sources on both sedimentary systems.

3.1 Baseline for estuaries from the Southwest of Spain

3.1.1 Granulometry

The granulometric analysis is very useful to have information on the predominant grain size for each sedimentary systems and, therefore, information on the predominant specific surface area of the grains presents in the samples, which favors the sorption of pollutants as the grain size decreases.

The granulometry distribution is very similar for most of the core samples, and an example of this distribution in Fig. A.2a (Supplementary Material – Appendix A) is shown (depth = 16 cm, Piedras River). Thus, it is possible to find a maximum at about 10 μm which suggests that a fine fraction is predominant, being the fine fraction (clay + silt) about 80% of the samples. However, it is also possible to find other two small relative maximums at about 300 μm and 500 μm, which suggests that coarse fractions are also present, especially in the deepest samples (52 cm), with about 40% of sand.

Then, in Fig. A.2b it is possible to observe the percentages of the different granulometric fractions obtained for the five selected samples of the core (depths = 2 cm, 16 cm, 30 cm and 52 cm) analyzed by laser diffraction in the case of the core taken from the Piedras River. As can be observed in Fig. A.2b, the silt fraction ranged from 54% (depth = 52 cm) to 88% (depth = 16 cm). However, it is also possible to observe a significant presence of the different types of sand, which is especially true for fine and medium sands that ranged from 3% (16 cm) to 29% (52 cm), and from 1% (16 cm) to 14% (52 cm), respectively. In addition, for 2 cm of depth, it is also possible to observe a significant contribution of coarse sand which was found to be about 10%.

Consequently, according to the results shown in Fig. A.2, it is possible to note that the presence of the coarse fraction is relative significant for all the samples excepting for depth = 16 cm.

3.1.2 Concentrations of major and trace elements

The concentrations of the major and trace elements were obtained for the different depths analyzed for the core taken from the Piedras River. As can be seen in Fig. 2, the concentrations obtained for the major elements are similar to those found in typical soils (Rudnick and Gao, 2003), where the concentrations of K, Na and Mg (Fig. 2a) were ranged from 1% to 2%, which are concentrations for typical soils. This is consistent with the granulometric analysis (see Fig. A.2), for which coarse fraction (fine sand + medium sand + coarse sand) was found to be relatively high, that is, the SiO_2 content must also be relatively high, as occurred for the Piedras River core. In the case of Fe and S (Fig. 2b), note that their concentrations ranged from 2% (52 cm) to 4.5% (30 cm), and from 0.3% (42 cm) to 1.8% (30 cm), respectively, are slightly higher than typical soils. This is consistent since the Piedras River basin contain some areas belonging to the Iberian pyrite belt (IPB), which is characterized by the presence of massive polymetallic sulphurs.

Furthermore, in Fig. 2b it is also possible to observe that the concentration of Al is relatively low at the deepest layers, as 52 cm of depth. This agrees well with the granulometric fractions obtained at 52 cm of depth, where contributions of fine and medium sands were found to be higher than those found for a typical soil. Therefore, the percentage of SiO_2 present at that depth is also higher than that found for a typical soil, making the Al concentration be lower than for a typical soil. Then, in the case of the Ti and P (Fig. 2c), no significant concentrations were found, which were less than 0.8% and 0.05%, respectively, for all the depths. In addition, note that for all the great majority of the major elements, two maximums (8 cm and 30 cm of depth) were observed which must correspond to a natural enrichment.

In the case of the trace elements (Figs. 2d, 2e and 2f), their concentrations were in general at the same order of magnitude that to the unperturbed sediments, which agrees well with the results obtained with major elements and granulometric fractions. There were only two exceptions, Cu and Zn, whose concentrations were ranged from 100 μg g^{-1} to 350 μg g^{-1}, and 100 μg g^{-1} to 600 μg g^{-1}, respectively. However, this is consistent with geographical location of the Piedras River, which is located near the IPB where massive polymetallic sulphurs are present. In addition, note that for the great majority of the trace elements, two maximums were also found for the same depths than those observed for major elements, which is consistent.

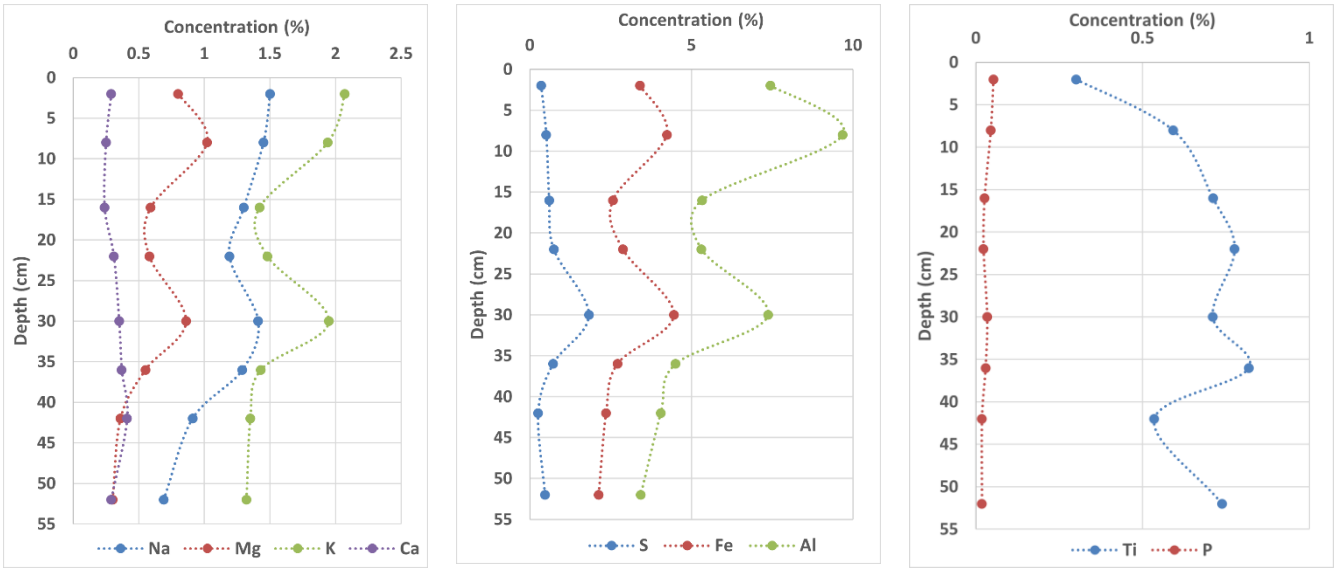

A B C

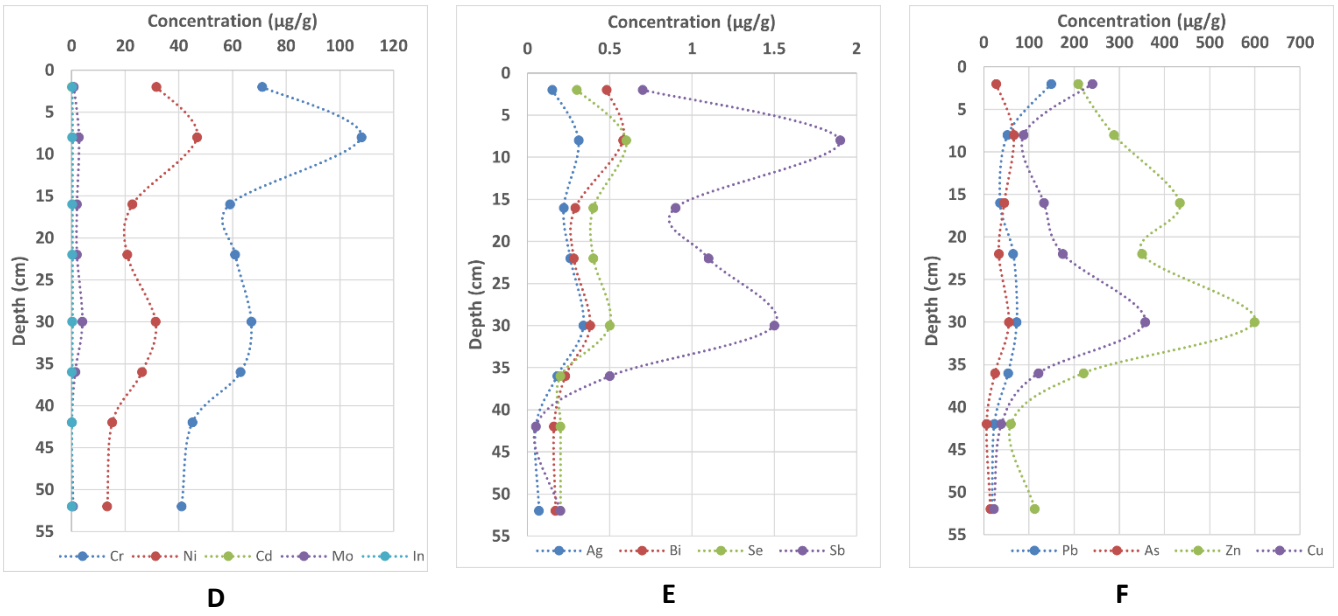

Fig. 2. Concentrations of both major (from A to C) and trace (from D to F) elements contained in the core taken from Piedras estuary.

253

254 ### *3.1.3 Concentrations of natural radionuclides*

255 In the case of the concentrations obtained for natural radionuclides (^{238}U-series, ^{232}Th-series and
256 ^{40}K) at the different depths considered for the core taken from the Piedras River, they were shown
257 in Fig. 3. As can be seen in Fig. 3a, the concentrations of the different radionuclides belonging to
258 the ^{238}U-series (^{238}U, ^{226}Ra and ^{210}Pb) were ranged from 21 Bq kg^{-1} to 46 Bq kg^{-1}, from 16 Bq kg^{-1}
259 to 27 Bq kg^{-1}, and from 17 Bq kg^{-1} to 41 Bq kg^{-1}, respectively. These concentrations agree well
260 with those found for typical soils (UNSCEAR, 2000). For ^{232}Th-series (^{228}Ra and ^{228}Th) and ^{40}K
261 (Fig. 3b), activity concentrations (20-37 Bq kg^{-1}, 24-40 Bq kg^{-1} and 373-789 Bq kg^{-1} for ^{228}Ra,
262 ^{228}Th and ^{40}K, respectively) were also found to be very similar to those present for typical soils.
263 This is very consistent with the concentrations obtained for stable elements (see Fig. 2) and
264 granulometric fractions (see Fig. A.2). Furthermore, in Fig. 3, it is also possible to observe
265 maximums of concentrations at about 8 cm and 30 cm, which agree well with those maximums
266 found for stable elements.

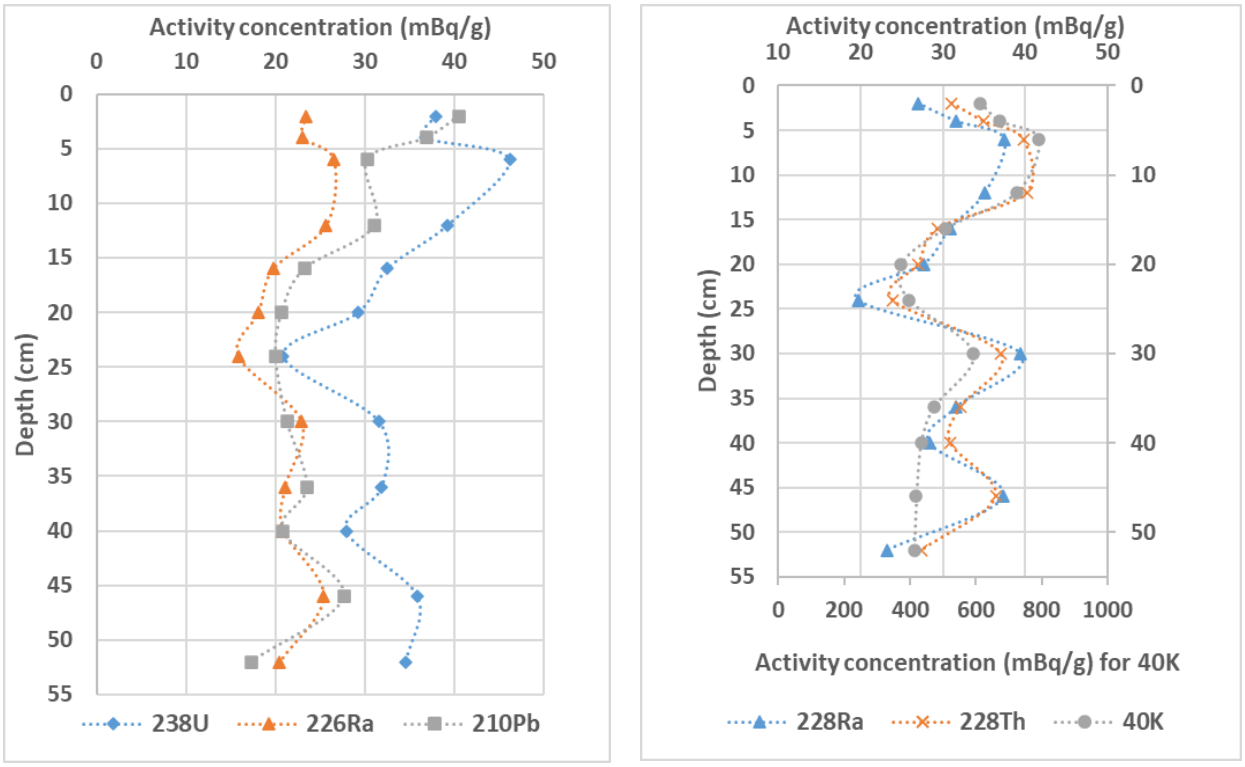

Fig. 3. Concentrations of radionuclides, belonging to the ^{238}U-series (A), and to the ^{232}Th-series and ^{40}K (B), present in the core taken from Piedras estuary.

3.1.4 Background assessment

To decide if the Piedras River can be considered as a proper sedimentary background (baseline), it is necessary to assess different types of pollution indexes (such as *EF* and *CF*) for stable elements and radionuclides, allowing us to make that decision. For this, it is necessary to use of the concentrations of the stable elements (heavy metals in this study) and radionuclides.

In the case of the enrichment factor, *EF*, it was calculated for the heavy metals and As. The *EF* obtained in our case were compared with those resulting from other sedimentary systems present in geographical regions close to the study area, being selected the estuaries of Formosa, Guadiana, Odiel and Guadalquivir for comparison with our reference area (Piedras estuary). Piedras River has been selected since previous works (Caliani et al., 1997; Lario et al., 2016) have demonstrated that no mining activities has been developed on its basin. In addition, for these sedimentary systems the data given by Rudnick and Gao (2003) for the mean of the upper earth crust was chosen as reference, and Al was considered as the normalizer element because of its conservative behaviour (Lee et al., 2021; Zhang et al., 2016). The *EF* for heavy metals and As were shown for the different sedimentary systems in Fig. 4. In our case, we distinguished two cases for our studied core, that is, Piedras-2 (two deepest samples) and Piedras-3 (entire core).

As can be seen in Fig. 4, *EF* was calculated in relation to Rudnick and Gao (2003) for different estuary systems. The *EF* obtained for great majority of the stable elements were less than 2. This result demonstrates that there is no significant pollution for any of them, where similar *EF* values

were found for all the cases. This is especially true when comparing our case (Piedras-2 and Piedras-3) with Piedras-1 (Lario et al., 2016) since the core Piedras-1 was taken from a region very close to that corresponding to the core selected for our study. Furthermore, note that in the case of Piedras-2, lower *EF* were achieved comparing with those resulting from Piedras-3. Therefore, Piedras River is a proper background, where Piedras-2 (average between the two deepest samples) is a more appropriate option, but the concentrations of all elements is not known, and for that we have taken the element concentrations of our study as baseline (background) of the estuaries located at the Southwestern Spain.

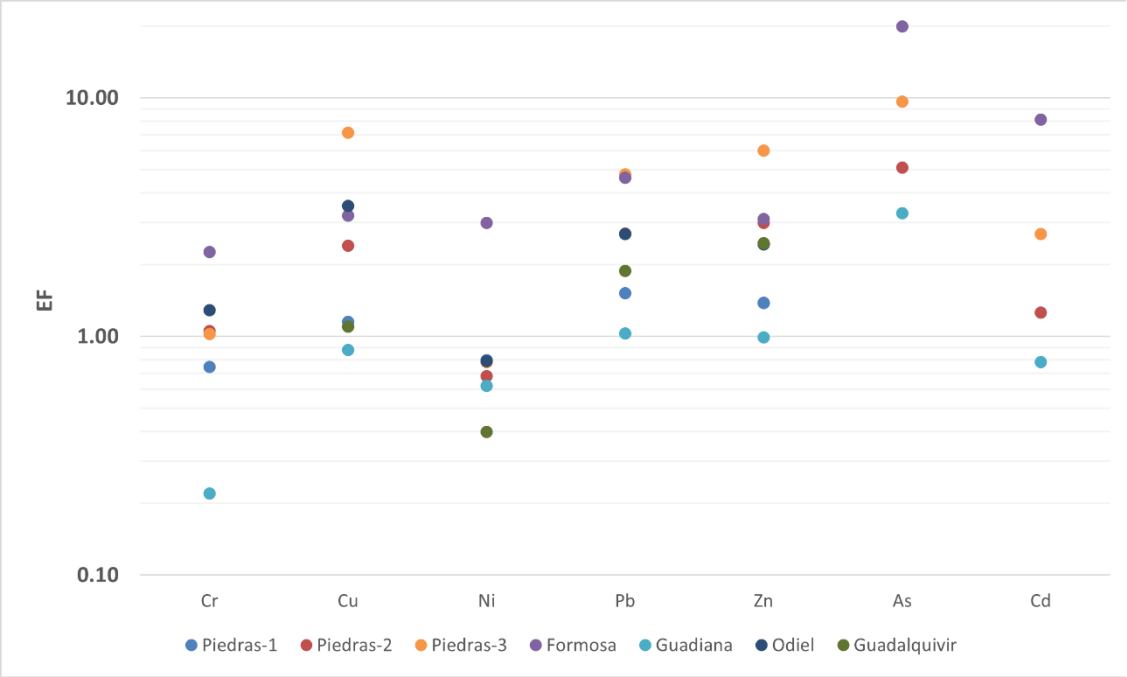

Fig. 4. Enrichment factors (*EF*) calculated in relation to Rudnick and Gao (2003) for different estuary systems. Piedras-1: Deep core (several meters) of Piedras estuary (Lario et al., 2016); Piedras-2: Core of Piedras estuary, considering the two deepest samples (this study); Piedras-3: Core of Piedras estuary, considering the entire core (this study); Formosa: Surface samples from Formosa estuary (Sousa et al., 2019); Guadiana: Surface samples from Guadiana estuary (Delgado et al., 2012); Odiel: Surface samples from Odiel estuary (Borrego et al., 2002); Guadalquivir: Surface samples from Guadalquivir estuary (Riba et al., 2002).

In the case of the natural radionuclides (^{238}U, ^{228}Ra, ^{228}Th and ^{40}K), *EF* and *CF* were calculated for the entire core, 12 samples (see Fig. A.3 in Supplementary Material – Appendix A). As can be seen in Fig. A.3a, the *EF* values were generally between 1 and 2, therefore, according to Table A.1, no significant pollution due to radioactivity was found. For further corroboration, *CF* was also obtained for the same radionuclides and depths than the previous ones, achieving *CF* values of 1.5 for the great majority of the cases (Fig. A.3b). Consequently, it is possible to conclude that the Piedras River is a proper background in our case for natural radionuclides in estuarine sediments from this geographical area.

In addition, to establish a proper baseline, numerical information of the concentrations of all the stable elements and radionuclides measured was included. In Table A.2 (see Supplementary Material – Appendix A), concentrations of major elements and radionuclides for all the depths

306 considered for this core can be consulted, as well as their average values and their respective
307 standard deviations (SD) and standard deviations of the average (SU). Analogously to Table A.2,
308 Table A.3 (see Supplementary Material – Appendix A) shows numerical information about the
309 concentrations of trace elements for all the considered depths, as well as their average values.
310 Thus, Table 1 shows the concentrations of major elements, natural radionuclides and trace
311 elements established as background values for the Piedras estuary core analyzed in this study. For
312 this, the average between the two deepest samples of the Piedras estuary core was considered (that
313 is, Piedras-2 in Fig. 4) since it is a more appropriate option as sedimentary background, as
314 previously demonstrated. In addition, the sedimentation rate of the Piedras core analyzed in this
315 study was obtained by the ^{210}Pb dating method (San Miguel et al., 2001),, obtaining a
316 sedimentation rate about 0.08 cm yr^{-1}, which shows that the age of its two deepest layers (42 cm
317 and 52 cm) is about 525 and 650 years, respectively. Consequently, since for those sediment ages
318 there was no pollution source, this further corroborates that the establishment of the sedimentary
319 background by using the Piedras River core analyzed in this study has been properly carried out.

Table 1

Concentrations of major elements (in %), natural radionuclides (in Bq kg^{-1}) and trace elements (in μg g^{-1}) established as background values for the Piedras estuary core analyzed in this study.

Na	Mg	Al	K	Ca	Fe	Ti	P	S	^{226}Ra	^{232}Th	^{40}K	
0.80	0.33	3.74	1.34	0.35	2.25	0.64	0.018	0.37	20.8	27.4	442	
Cd	Cr	Ni	Ag	Bi	Se	Zn	As	Mo	In	Sb	Cu	Pb
< 0.1	43	14	0.06	0.17	0.20	87	11	0.36	< 0.1	0.13	21	31

320 At a national level, the Spanish Royal Decree 9/2005 establishes the guideline levels for
321 contaminated soils that require remediation measurements are those with heavy metal
322 concentrations over 100-times baseline values (Royal Decree, 2005). No studies have been carried
323 out to assess the base line of the estuaries located at the Southwestern Spain for major elements,
324 trace elements, metalloids and rare earth elements. Therefore, in Section 3.1.5 additional analysis
325 are carried out to further verify that the Piedras River core used in this work is not impacted.

326 ***3.1.5 Correlation analysis and pollution sources***

327 To find possible contributions of the different potential pollution sources existing in this
328 geographical area (AMD, industries, wastewaters releases, etc.), a correlation analysis was
329 accomplished between the different stable elements. The criteria followed for the selection of
330 these elements was a obtain a significant correlation coefficient at level of 0.05, and R higher than
331 |0.8|. The spearman correlation matrix in Supplementary Material – Appendix B has been
332 included, and the plots of the most relevant correlations in Fig. A.4 (see Supplementary Material
333 – Appendix A) have been included.

334 As can be seen in Fig. A.4, the correlation between Mg and Fe is positive. In the case of the
335 Piedras River, the Mg is a naturally occurring element. This suggests that for the Piedras River,
336 an enrichment of Fe is also naturally occurring, which is consistent given that Piedras River is not
337 significantly affected by pollution sources as proven in Sections from 3.1.2 to 3.1.4, existing only
338 natural enrichments due to the mixing of seawaters with the fluvial ones. In the case of the Th and
339 Fe, analogous behavior to the previous one was found, that is, a positive correlation. Therefore,
340 this suggests that Th is naturally enriched since Fe was proven not to be contributed by no

pollution source in the case of the Piedras River. Then, for the As-Fe pair, it also possible to observe a positive relationship, which is consistent given that the Piedras River is located near the Iberian pyrite belt. Therefore, the As is naturally present due to the massive polymetallic sulphurs. Note that Fe was selected for these three cases because of being the tracer of the pollution coming from AMD. Consequently, no impact generated by AMD was found in the case of the Piedras River.

Then, as it has been demonstrated in previous studies (Bolívar et al., 2009), the P element is a very good marker of the pollution coming from fertilizers industry releases. Thus, in Fig. A.4, U, Bi and Pb were plotted versus P, achieving positive correlations for the three cases. This means that U, Bi and Pb are naturally enriched since Piedras River is not affected by PGL.

Then, it is interesting to highlight that the correlation between Fe and P was also relatively high (R = 0.71, see Supplementary Material – Appendix B), which can be explained due to both elements are naturally enriched, therefore both are similar origin in the case of the Piedras River.

3.2 Odiel estuary

Once the background has been established and its suitability was proven, it is possible to assess the environmental impact in the Odiel River channel. For this, an order analogous to Section 3.1 was followed when applying the different analysis techniques.

3.2.1 Granulometry

As can be seen in Fig. A.5a (see Supplementary Material – Appendix A), an example of granulometric curve (depth = 42 cm) was shown for the core taken from the Bacuta Island. Thus, a maximum for a grain size slightly higher than 10 μm is found, which proves that fine fraction (silt in this case) is predominant. Another maximum at about 1000 μm is also possible to observe, which is related to coarse fraction (coarse sand in this case), but its contribution can be neglected comparing with that found for fine fraction.

In the case of Fig. A.5b, two fractions were clearly predominant: silt and fine sand. For silt, the granulometric fractions ranged from 61% (depth = 2 cm) to 84% (depth = 42 cm) and for fine sand and, they were between 8% (depth = 42 cm) and 22% (depth = 2 cm). For all the other granulometric fractions, their respective percentages were less than 5% for the great majority of the cases. Considering the relative high percentage of fine fraction at 42 cm of depth (almost 90% considering silt + clay), it suggests that it is very likely to find a maximum of concentrations of the different pollutants (trace elements and radionuclides) at about that depth.

3.2.2 Concentrations of major and trace elements

As can be seen in Fig. 5, the concentrations of major elements (Figs. 5a, 5b and 5c) and trace elements (Figs. 5d, 5e and 5f) were shown for the different depths considered in the case of the core taken from Bacuta Island, having selected the same stable elements than those analyzed for the Piedras River (see Fig. 2 in Section 3.1.2). In addition, the concentrations of major elements and trace elements can be consulted in Tables A.4 and A.5, respectively (Supplementary Material – Appendix A).

For Na, Mg, K and Ca (Fig. 5a), they have similar behaviors than those found for Piedras River (see Fig. 2a), that is, they are relatively stable along all the sediment core, and all these elements have concentrations very similar for both sedimentary systems along all vertical profiles. This is consistent since these are naturally present in both sedimentary systems. For Na, it is possible to

observe a slight increase at superficial layers, which could be due to the contribution of seawater contained in the pores of the sediments. Then, in the case of Fe and S (Fig. 5b), they have concentrations relatively higher than those found for Piedras River (see Fig. 2b), that is, about 2-7 times and 2-6 times, respectively. These relatively high concentrations can be due to the significant affection of AMD in Bacuta Island, where Fe can be used as a tracer of AMD influence. In the case of Fig. 5c, very similar behaviors and concentrations were obtained for Ti when comparing with the core taken from Piedras River (see Fig. 2c). This suggests that Ti is naturally present in both sedimentary systems.

However, in the case of P, note that its concentrations are about one order of magnitude higher than those obtained for Piedras River, excepting the three deepest samples. This is due to the influence of the industrial production of phosphoric acid that began around the year 1965 in the surroundings of Huelva city. In this case, the pollution is caused indirectly since the P is dissolved in the phosphogypsum leachates (PGL), since the PG was pumped into the Odiel Channel in suspension of seawater (20% of PG + 80% of seawater), being P mainly in dissolution due to its very high solubility in acid water (pH = 1-2) (Guerrero et al., 2019). Thus, P can be used as a very good tracer/marker of the pollution coming from the phosphogypsum piles and the releases of the phosphoric acid plants. In Fig. 5c, a significant increase of the P concentration up to 45 cm is observed, demonstrating this fact the impact of the phosphoric acid plants and PG leachates in this area and being possible to relate the maximum of P concentration at about 44 cm with the beginning of the industrial activity of the production of phosphoric acid, that is, about the year 1965.

Then, in the case of the trace elements (Figs. 5d, 5e and 5f), the same stable elements than those studied in Section 3.1.2 were analyzed. For Cr, Ni, Cd, Mo and In (Fig. 5d), similar concentrations were obtained with respect to Piedras River (see Fig. 2d). However, note that in the case of the Bacuta Island core, maximum concentrations for these elements were generally obtained at 14 cm, 22 cm and 42 cm of depth. This agrees well with the granulometric results (see Fig. A.5b), where the pollution level seems to be increased as the percentage of fine fraction (clay + silt) increases, finding maximums of fine fraction at 16 cm, 26 cm and 42 cm.

For Ag, Bi, Se and Sb (Fig. 5e), concentrations were about one order of magnitude higher than those found in Piedras River (see Fig. 2e). In addition, note that their behaviors are very similar from each other, and they are also similar to that obtained for P. This suggests that these four elements can be provided by PGL.

Then, in the case of the Pb, As, Zn and Cu (Fig. 5f), their concentrations are about one order of magnitude higher than those obtained for Piedras River (see Fig. 2f). For Pb, it is possible to observe a similar behavior than P, finding three maximums (14 cm, 26 cm and 42 cm). This means that Pb can come from releases of phosphogypsum piles. For the rest of elements, As, Zn and Cu, the relative high concentrations can be partially due to the AMD influence, which is consistent since they are toxic elements usually present in massive polymetallic sulphurs. In this case, this is especially true for As which follows a behaviour very similar to Fe (Fig. 5b).

However, note that the concentrations of all elements decreased significantly at the highest depths (> 55 cm). This is consistent since the layers at those depths may have been formed before starting the mining activity, that is, before the second half of XIX century. Therefore, the concentrations of all elements tend to be similar to those obtained for unpolluted soils (Rudnick and Gao, 2003).

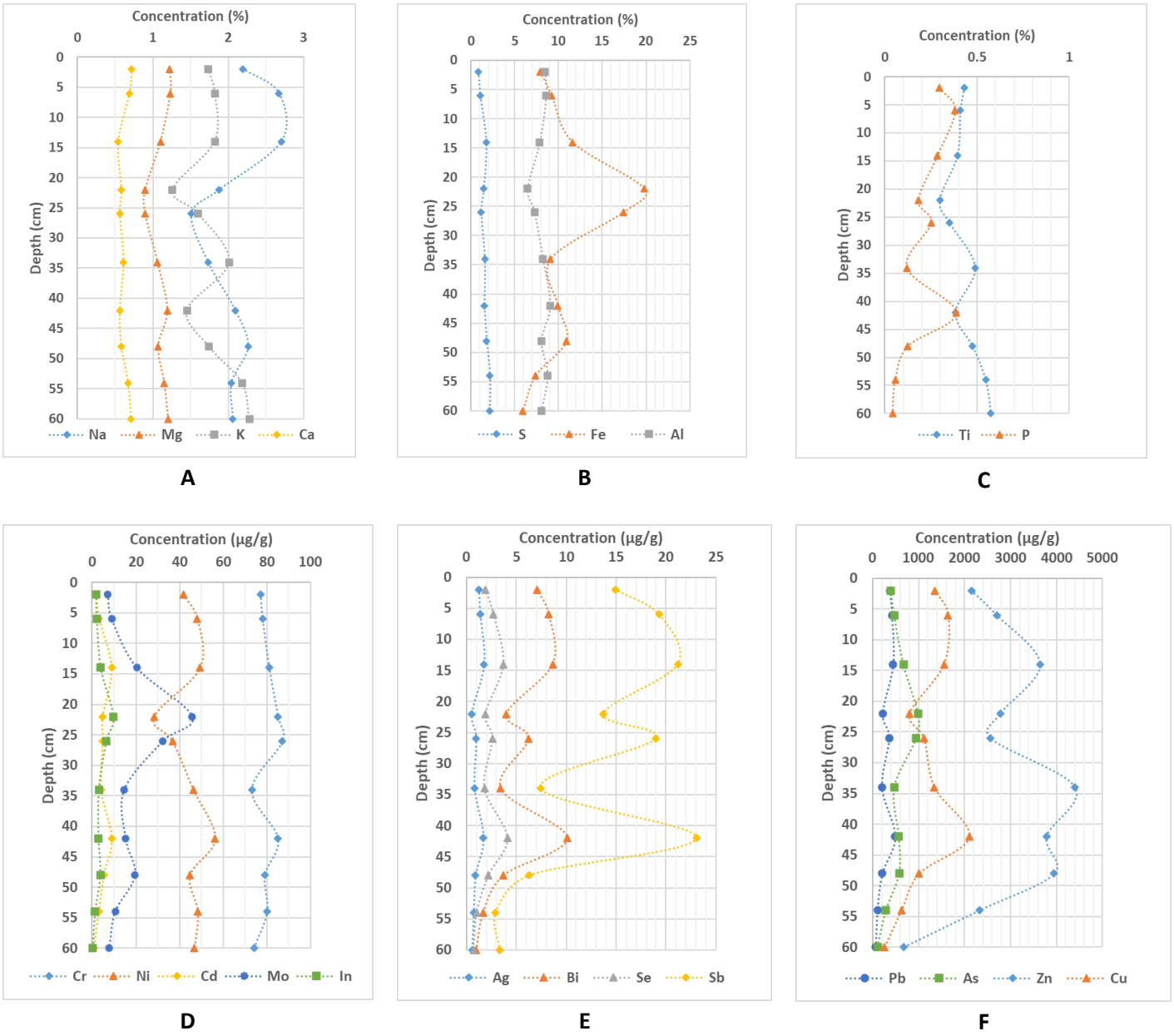

Fig. 5. Concentrations of major (from A to C) and trace (from D to F) elements present in the core taken from Bacuta Island.

426

427 ### *3.2.3 Concentrations of natural radionuclides*

428 With respect to the behaviors and activity concentrations of the natural radionuclides along the
429 core taken from Bacuta Island, in Fig. 6 the concentrations of the radionuclides belonging to the
430 ^{238}U-series (^{238}U, ^{226}Ra and ^{210}Pb) (Fig. 6a), and ^{232}Th-series (^{228}Ra and ^{228}Th) and ^{40}K (Fig. 6b)
431 are shown. In addition, these concentrations of radionuclides can be consulted in Table A.6
432 (Supplementary Material – Appendix A). As can be seen in Fig. 6a, the ^{238}U concentration pattern
433 is like that previously found for P (see Fig. 5c), and in the next section will be ratified by the high
434 correlation coefficient existing between both elements U vs P. This is consistent since U source
435 also comes from the phosphoric acid industry and PG piles and given that P and U are very mobile
436 elements, they must follow a very similar behavior/pattern. On the contrary, both ^{226}Ra and ^{210}Pb

437 also come from phosphoric acid industry but they are very reactive, i.e., they tend to be bound to
438 the particulate material, and they also follow a similar pattern along the core. In addition, note
439 that the activity concentrations of ^{238}U, ^{226}Ra and ^{210}Pb are much higher than those obtained for
440 the Piedras River, therefore Bacuta Island is significantly affected by PGL.

441 For ^{232}Th-series (^{228}Ra and ^{228}Th) and ^{40}K (Fig. 6b), it is possible to observe that they are
442 concentrations very uniform along the core (around 30 Bq kg^{-1}), and similar to those found for
443 typical soils (UNSCEAR, 2000). This is consistent since in this case, no pollution sources for Th-
444 series radionuclides are affecting to this area, therefore they are naturally present in this
445 sedimentary system. The ^{232}Th activity concentration can be calculated from the Th ICP-MS
446 measurements and the relation ^{232}Th (Bq/kg) = 4.05 Th (mg/kg), finding and average of 38 Bq/kg,
447 which is very similar to the ^{228}Ra one, so ^{232}Th-series radionuclides are in secular equilibrium as
448 it is expected in unperturbed estuarine sediments.

449 In the case of the Bacuta Island core, due to the clear anthropogenic impact, it was necessary to
450 apply the methodology developed by San Miguel et al. (2001), where the $^{230}Th/^{232}Th$ activity ratio
451 was previously calculated and plotted versus the depth (see Fig. A.9 in Supplementary Material –
452 Appendix A) in order to decide for which depth interval is possible to apply the ^{210}Pb dating
453 method. Thus, to make use of the ^{210}Pb dating method, the $^{230}Th/^{232}Th$ activity ratio needs to be
454 about 1 in order to avoid possible additional contributions of ^{210}Pb that can cause that the
455 unsupported ^{210}Pb cannot be properly calculated by using the equation: a(unsupported ^{210}Pb) =
456 a(supported ^{210}Pb) – a(^{226}Ra), where a(unsupported ^{210}Pb), a(supported ^{210}Pb) and a(^{226}Ra) are the
457 concentrations of unsupported ^{210}Pb, supported ^{210}Pb and ^{226}Ra, respectively. Thus, as can be seen
458 in Fig. A.9, the $^{230}Th/^{232}Th$ activity ratio was stable and about 1 from depths > 50 cm. Therefore,
459 since the concentrations of unsupported ^{210}Pb are very low from depths > 50 cm, it was not
460 possible to apply the ^{210}Pb dating method in the case of the Bacuta Island core. However, since
461 the $^{230}Th/^{232}Th$ activity ratio behavior was very similar to the behavior found for the vertical
462 profile of ^{238}U concentrations (Fig. 6a), it was possible to further corroborate that the depth of
463 about 44 cm corresponds to the beginning of the industrial activity of the acid phosphoric
464 production in Huelva, that is, the year 1965. Consequently, for the polluted part of the Bacuta
465 Island core, it was possible to establish a sedimentation rate of about 0.8 cm yr^{-1}.

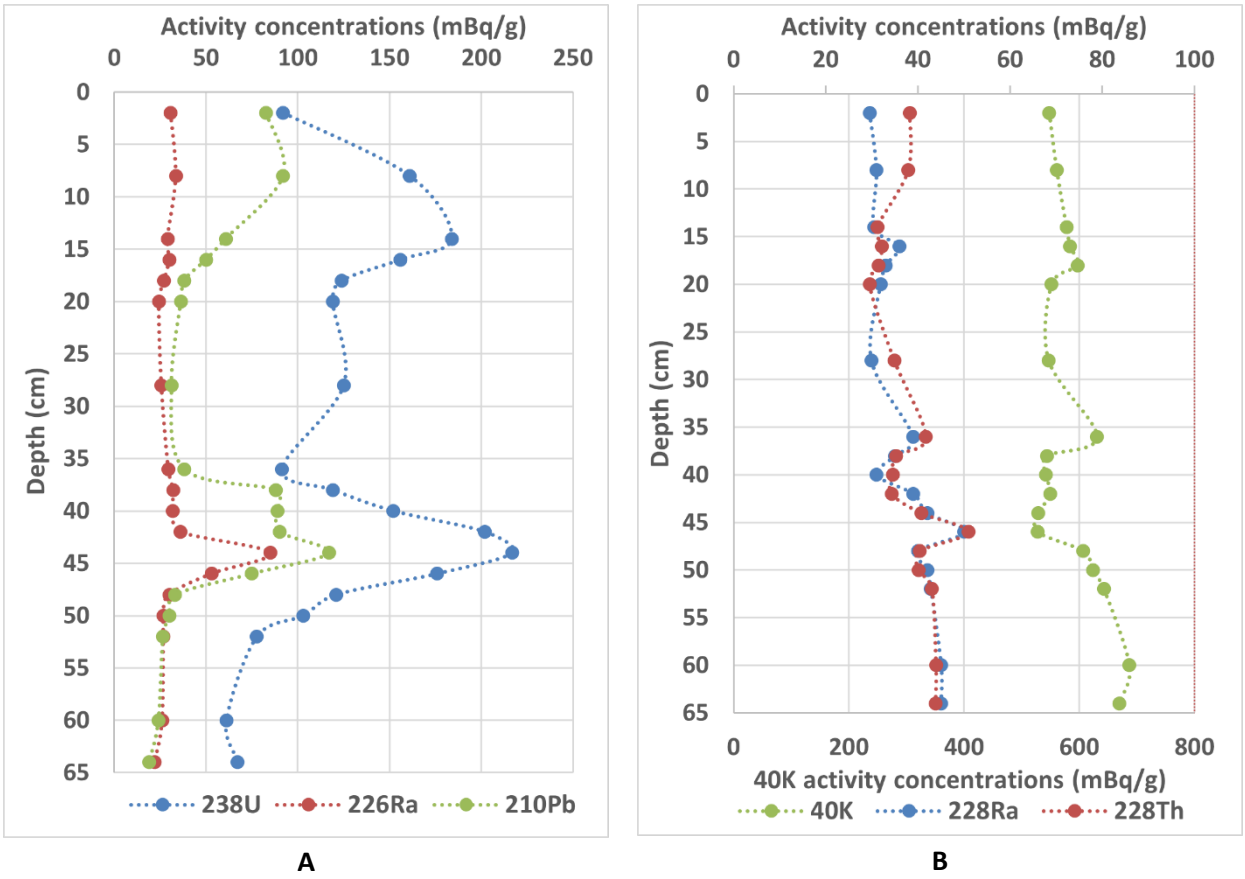

Fig. 6. Concentrations of radionuclides, belonging to the ^{238}U-series (A), and to the ^{232}Th-series and ^{40}K (B), present in the core taken from Bacuta Island.

3.2.4 Pollution indexes

Once the concentrations of all stable elements and radionuclides of interest have been determined in the case of Bacuta Island core, and the sedimentary background has been properly established (by considering the two deepest layers of our Piedras River core, see Table 1), it is possible to calculate the different pollution indexes in order to assess the environmental impact in the Bacuta Island.

In the case of the *EF* for major elements, as can be seen in Figs. A.6a and A.6b (see Supplementary Material – Appendix A), the *EF* values for Na, Mg, K, Ca and Ti were less than 2, proving that there is no pollution associated to these major elements and they are naturally present in Bacuta Island. In addition, note that for S, *EF* was also less than 2 along the sediment core. However, it is necessary to clarify that it does not mean that there is no pollution related to poly-sulphide minerals mining from the basins of the Odiel and Tinto Rivers. Due to the sulphur travels in dissolution as sulphate anion ($SO4^{2-}$), this anion is very conservative during the mixing of the fluvial waters and seawater, and therefore it does not precipitate during these waters mixing and finally goes into the Atlantic Ocean, but the majority of Fe precipitates during the waters mixing process (Hierro et al., 2013; Nieto 2013; Nieto 2007). For P and Fe (Fig. A.6c), the great majority of *EF* values were higher than 2, which was especially true for P. This is consistent since affections due to PGL and AMD are significantly present in Bacuta Island, where P and Fe are the main tracers of these pollution sources, respectively.

Then, regarding the *CF* for the same major elements previously analyzed (Figs. A.6d, A.6e and A.6f), it is possible to observe that results analogous to those related to *EF* were obtained, where significant affection was mainly found for P and Fe (*CF* = 2-21 and *CF* = 2-9, respectively), which correspond to the pollution sources PGL and AMD, respectively.

With respect to the *EF* for trace elements (Figs. 7a, 7b and 7c), for Ag, Se, Bi and Sb (Fig. 7a), the *EF* values were higher than 5 for all these elements at depths less than 48 cm. The fact of obtaining relatively high *EF* values for these four elements is consistent since they are mainly provided by PGL as previously proven (Section 3.2.2). Therefore, given that the industrial production of phosphoric acid began in 1965, for depths higher than about 50 cm, there is no significant contribution of this type of pollution source. In the case of the In, Mo, As and Zn (Fig. 7b), they are mainly contributed by AMD, obtaining *EF* values higher than 10 for all the elements at any depth, excepting for surface sediments (0-5 cm of depth) and for deepest sediments (55-60 cm of depth). Then, for Pb, Cu, Cd, Cr and Ni, the *EF* values were higher than 10, excepting for Cr and Ni, for which *EF* were close to 1 along the entire core, and excepting at the deepest layers, where the *EF* for Pb, Cu and Cd decreased significantly.

In the case of the *CF* for trace elements (see Figs. A.6g, A.6h and A.6i in Supplementary Material – Appendix A), results analogous to those found for *EF* were obtained, where all *CF* were generally higher than 5 for all the elements, excepting for Cr and Ni, for which *CF* were very stable and about 1.5 and 2-4, respectively, for the entire core. Furthermore, at deepest sediments, that is, about 60 cm of depth, *CF* was generally $\lesssim 3$, therefore the pollution was moderate only at about that depth.

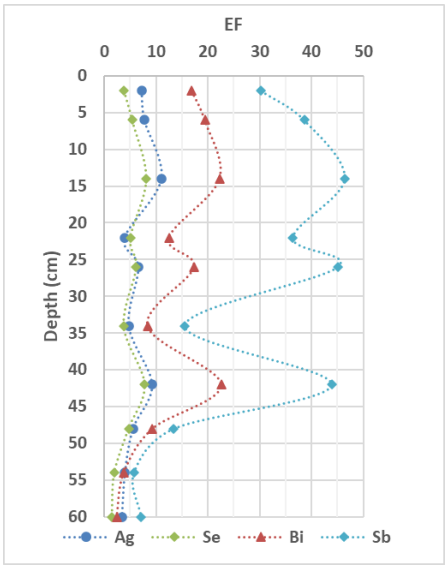

A

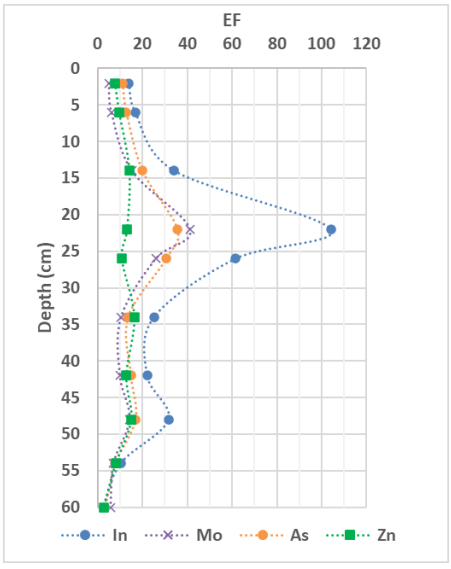

B

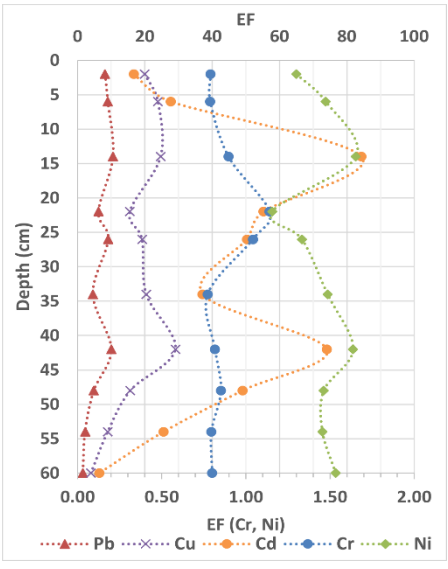

C

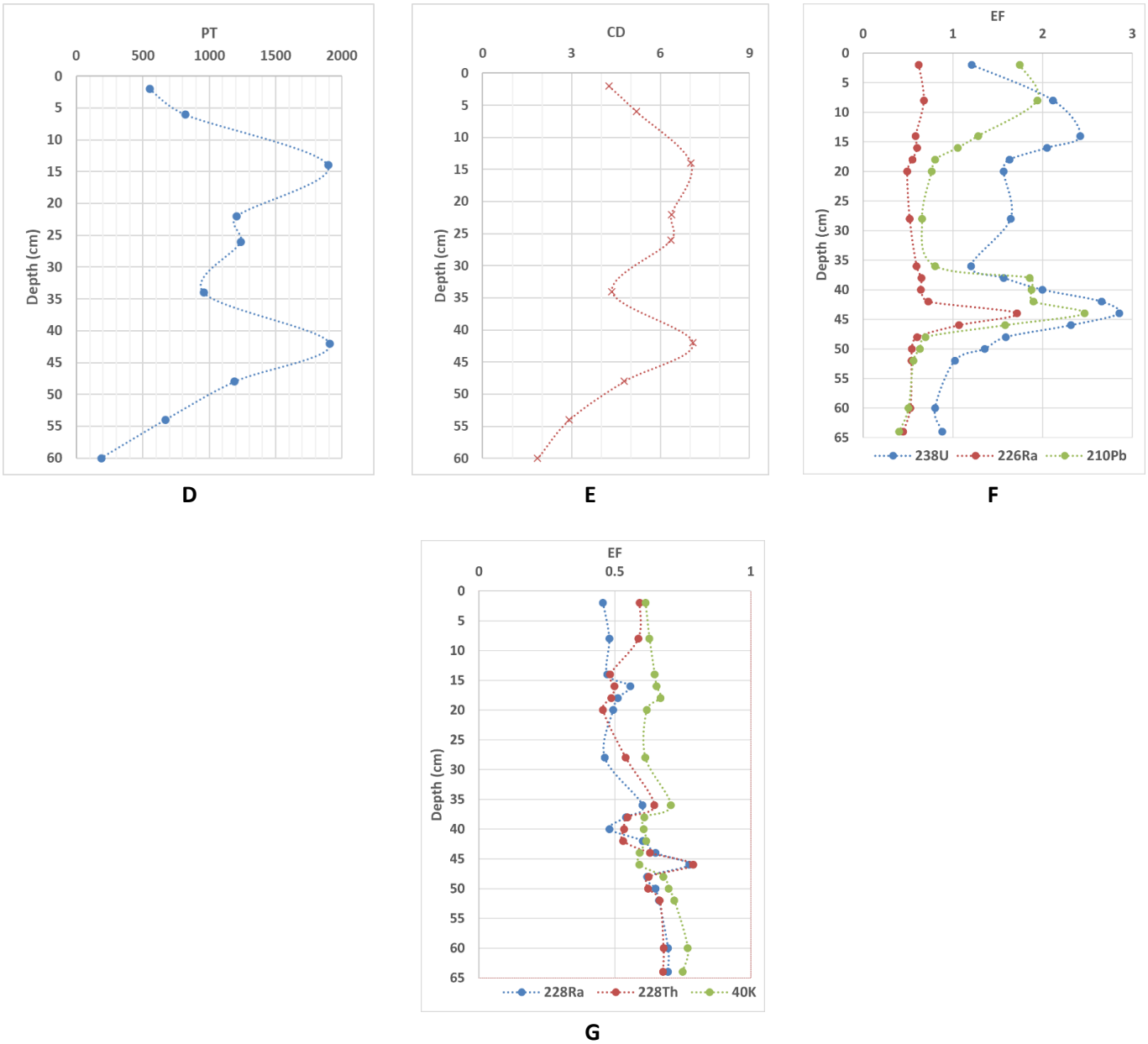

Fig. 7. Enrichment factor (*EF*) (from A to C), potential toxicity (*PT*) (D) and contamination degree (*CD*) (E) obtained for the trace elements in the case of the core taken from Bacuta Island, where *EF* calculated in relation to the two deepest samples of the core taken from Piedras estuary (see Table 1), considering the Al as the normalizer element in the case of the *EF* calculations. The *EF* was also obtained for radionuclides (F and G).

In the case of the elements of interest from a toxicological point of view, that is, the heavy metals and As, the index "potential ecological risk", *PER*, was assessed for each element along the core. As can be seen in Fig. A.7 (see Supplementary Material – Appendix A), all the *PER* values were less than 40 ($PER < 40$, that is, low pollution), excepting for As and Cd, which is especially high for Cd, where Cd and As are mainly generated by PGL and AMD, respectively.

When the *PT* and *CD* indexes are calculated for the different samples of the core (Figs. 7d and 7e, respectively), it is expected they follow the same pattern that Cd since its toxicity factor (T_i) is very much higher than those for the rest of toxic elements. Thus, when using the *PT* index (see Table A.1), it is observed a "serious" ($300 \leq PT < 600$) and "very serious" ($PT \geq 600$) ecological

risks for all the depths excepting for the deepest one, that is, at 60 cm, where the pollution was low. Then, when using the *CD* index (see also Table A.1), "high grade of pollution" was found for all the depths, excepting for depth ≥ 55 cm, for which the pollution was moderate.

In addition, the *EF* index was also assessed for natural radionuclides in the case of the core taken from Bacuta Island (Figs. 7f and 7g), as well as the *CF* index (see Figs. A.6j and A.6k in Supplementary Material – Appendix A). For the radionuclides belonging to the ^{238}U-series, the *CF* was ranged from 2 to 6 for ^{238}U, while for ^{210}Pb, the *CF* also reached a maximum of about 6, but lower values than for ^{238}U were achieved for the great majority of depths (Fig. A.6j). This is consistent since ^{210}Pb has a mobility much lower than the ^{238}U one. Then, the *CF* for ^{226}Ra was generally ≤ 2, excepting at 44 cm, which is logical since ^{226}Ra has a mobility lower than the ^{210}Pb one. In addition, note that the behavior of the *CF* index agrees with that resulting from the activity concentrations analyzed in Section 3.2.3 (Fig. 6) as expected, finding maximums of *CF* at 10-14 cm, 28 cm and 44 cm. In the case of the ^{232}Th-series (^{228}Ra and ^{228}Th) and ^{40}K (Fig. A.6k), the *CF* was ranged from 1 to 1.5, that is, no pollution was found due to these radionuclides, therefore they are naturally present in this sedimentary system. Regarding the *EF* index (Figs. 7f and 7g), the *EF* was higher than 2 only for ^{238}U at 14 cm and 44 cm of depth, and for ^{210}Pb at 44 cm. Then, for ^{232}Th-series and ^{40}K, the *EF* was less than 2 for the entire core, which is consistent with the *CF* values previously obtained for these radionuclides.

3.2.5 Correlation analysis and pollution sources

In this Section will be analyzed the different pollution sources making usage of the correlations between the different major and trace elements. Thus, according to the criteria mentioned in Section 3.1.5, several cases of high correlations were shown in Fig. A.8 (Supplementary Material – Appendix A). In the case of the couple Mg-Fe, the correlation was negative, which is the opposite case than that found for the Piedras River (see Section 3.1.5), which can be due to different basic mechanisms. Therefore, given that the Mg is naturally present in Bacuta Island, this means that Fe is being contributing anthropically, where AMD is pollution source in this case. In the case of Th, as was shown in Sections 3.2.3 and 3.2.4, the presence of Th is of natural type. Since the relationship between Th and Fe is negative, it further corroborates that Fe comes from AMD contribution. Then, for the case As-Fe, given that Fe is the tracer of AMD, and their correlation is positive, it suggests that As comes mainly from the contribution of a pollution source, which is AMD in this case as shown in Section 3.2.2 (Fig. 5).

On the contrary, in the case of the P, it is possible to observe that U, Bi and Pb have positive and linear correlations, but they have no significant correlations with Fe (see correlation matrix in Supplementary Material – Appendix B). This demonstrates that these three elements come mainly from the fertilizers plants activities since P is considered as the tracer of pollution coming from them.

In Supplementary Material – Appendix B, it is possible to observe the Principal Component Analysis (PCA) carried out for Bacuta Island. Thus, in the biplot of the principal components F1 and F2, the positive axis of F1 can be identified as the affection coming from the fertilizer industry since P can be found in this axis, while Fe can be found in the positive axis of F2, thus this axis represents the influence of AMD. Thus, in the positive axis of F1, it is possible to find elements such as U, Bi and Pb, while in the positive axis of F2, As is present. This corroborates the analysis previously carried out to find the pollution sources for these four elements.

Then, the correlation between Fe and P was found to be not significant (see Supplementary Material) since these two elements come from different pollution sources in the case of the Bacuta Island as previously demonstrated (AMD and fertilizer industry, respectively). This behavior is opposite to that found for the Piedras River (see Section 3.1.5), which is consistent.

4. Conclusions

An assessment of the environmental impact exiting in the estuarine biosphere reserve from the Southwestern Iberian Peninsula was carried out. For this, a suitable sedimentary background was assessed for evaluating the affection existing in this biosphere reserve generated by the fertilizer complex located in the Huelva estuary, that is, between the Tinto and Odiel Rivers.

The following main conclusions have been found from this study:

1. The enrichment factor (*EF*) and contamination factor (*CF*) were calculated for heavy metals and natural radionuclides in the case of the Piedras River, achieving *EF* and *CF* values very close to 1 for all the cases. This proves that the Piedras River is a proper sedimentary background in our case.

2. Regarding the core taken from both Piedras estuary and Bacuta Island, it was possible to observe that clay and silt were the predominant granulometric fractions for both ecosystems. This fact demonstrates Piedras estuary is a good reference area for Odiel estuary, finding a maximum percentage of clay + silt of about 90%.

3. P and Fe were the elements whose concentrations highlighted, observing a clear indirect affection of phosphogypsum piles by means of their leachates (PGL), and the impact of acid mine drainage (AMD). Thus, P and Fe were suitable to trace the pollution coming from PGL and AMD, respectively.

4. Then, several trace elements such as Bi, Pb, Se and Sb had concentrations quite higher (about 1 order of magnitude) than those obtained for the Piedras River. These elements followed a very similar behavior than that followed by P, therefore they were mainly contributed by PGL. For As, Cu and Zn, concentrations of about 1 order of magnitude higher than those found for the Piedras River were also obtained, where the main pollution source for these elements was AMD since their behaviors were similar to the Fe one.

5. In the case of radionuclides belonging to the ^{238}U-series, a clear impact by PGL was observed, and not from AMD. For radionuclides belonging to the ^{232}Th-series and ^{40}K, very stable concentrations were found along the entire core, and they were similar to those related to unpolluted soils.

6. The pollution indexes *EF* and *CF*, as well as the potential ecological risk, *PER*, reached in Bacuta Island values of serious and very serious pollution for the great majority of trace elements, as well as Fe and P, but observing that in the deepest sediments (more than 50 cm depth), the pollution was much less significant, which became moderate. This dependence of the pollution on depth was possible to be observed by using the potential toxicity, *PT*, and the contamination degree, *CD*. Then, *EF* and *CF* were used for natural radionuclides, observing low-moderate pollution for radionuclides belonging to the ^{238}U-series, and no pollution in the case of the ^{232}Th-series and ^{40}K.

Acknowledgments

This research was partially funded by the University of Huelva and the Operative FEDER Program-Andalusia 2014-2020 (UHU-1255876, UHU-202020); The European Regional Development Fund through the Spanish Ministry of Science, Innovation and Universities' Research Agency (research grants PID2020-116461RB-C21 and 116461RA-C22); and the Andalusian government (I+D+i-JAPAIDI-Retos, project Ref.: PY20_00096, and Diagnosis and proposals for the environmental recovery of areas affected by industrial and mining activities; Implications for the Huelva estuary (RESTOREHU), Ref.: TED2021-130361B-I00). José Luis Guerrero thanks the Spanish Ministry of Universities for the Margarita Salas research grant.

References

Aduvire, O. (2006). Drenaje ácido de mina generación y tratamiento. Dirección de Recursos Minerales y Geoambiente, Instituto Geológico y Minero de España, Madrid, 140 pp.

Barba-Lobo, A., San Miguel, E. G., Lozano, R. L., & Bolívar, J. P. (2021a). A general methodology to determine natural radionuclides by well-type HPGe detectors. Measurement, 181, 109561. https://doi.org/10.1016/j.measurement.2021.109561.

Barba-Lobo, A., Mosqueda, F., & Bolívar, J.P. (2021b). An upgraded Lab-based method to determine natural γ-ray emitters in NORM samples by using Ge detectors. Measurement, 186, 110153, https://doi.org/10.1016/j.measurement.2021.110153.

Bolívar, J. P., Martín, J. E., García-Tenorio, R., Pérez-Moreno, J. P., & Mas, J. L. (2009). Behaviour and fluxes of natural radionuclides in the production process of a phosphoric acid plant. Applied Radiation and Isotopes, 67(2), 345–356. https://doi.org/10.1016/j.apradiso.2008.10.012.

Bolívar, J. P., García Tenorio, R., & M. Matarranz, J. L. (2008). Evaluación radiológica del apilamiento de fosfoyesos de las marismas del río Tinto (Huelva).

Bolívar, J.P., García-Tenorio, R., & Garcia-Leon, M. (1995). Enhancement Of Natural Radioactivity In Soils And Saltmarshes Surrounding A Non-Nuclear Industrial Complex. Science of the Total Environment 173, 125-136.

Borrego, J., Morales, J. A., De la Torre, M. L., & Grande, J. A. (2002). Geochemical characteristics of heavy metal pollution in surface sediments of the Tinto and Odiel river estuary (southwestern Spain). Environmental Geology, 41(7), 785–796. https://doi.org/10.1007/s00254-001-0445-3.

Caliani, J.C., Ruíz, F., & Galán, E. (1997). Clay mineral and heavy metal distributions in the lower estuary of Huelva and adjacent Atlantic shelf, SW Spain. Science of The Total Environment, 198, 181-200. https://doi.org/10.1016/S0048-9697(97)05450-8.

Curcio, A. C., Barbero, L., Casas-Ruiz, M., & López-Ramírez, J. A. (2019). Fractionation of U and heavy metals into the colloidal fraction in acid mine drainage conditions in the Río Tinto area (SW Spain). Journal of Contaminant Hydrology, 222, 65–75. https://doi.org/10.1016/j.jconhyd.2019.02.008.

Delgado, J., Boski, T., Nieto, J. M., Pereira, L., Moura, D., Gomes, A., Sousa, C., & García-Tenorio, R. (2012). Sea-level rise and anthropogenic activities recorded in the late Pleistocene/Holocene sedimentary infill of the Guadiana Estuary (SW Iberia). Quaternary Science Reviews, 33, 121–141. https://doi.org/10.1016/j.quascirev.2011.12.002.

Díaz-Asencio, M., Corcho Alvarado, J.A., Alonso-Hernández, C., Quejido-Cabezas, A., Ruíz-Fernández, A.C., Sánchez-Sánchez, M., Gómez-Mancebo, M.B., Froidevaux, P., & Sánchez-Cabeza, J.A. (2011). Reconstruction of metal pollution and recent sedimentation processes in Havana Bay (Cuba): A tool for

coastal ecosystem management. Journal of Hazardous Materials, 196, 402-411. https://doi.org/10.1016/j.jhazmat.2011.09.037.

García-Tenorio, R. & García-León, M (1996). Radioactive impact of some phosphogypsum piles in soils and salt marshes evaluated by γ-ray spectrometry. Applied Radiation and Isotopes 47 (9-10), 1069-1075.

Gázquez, M. J., Bolívar, J. P., García-Tenorio, R., & Galán, F. (2009). NATURAL OCCURRING RADIONUCLIDE WASTE IN SPAIN: THE HUELVA PHOSPHOGYPSUM STACKS CASE. 1st Spanish National Conference on Advances in Materials Recycling and Eco – Energy. Madrid, 12-13 November 2009. pp. 75-78.

Gözel, F., Belivermis, M., Sezer, N., Kurt, M.A., Sikdokur, & E., Kilic, Ö. (2022). Chronology of trace elements and radionuclides using sediment cores in Golden Horn Estuary, Sea of Marmara. Environmental Pollution, 315, 120359. https://doi.org/10.1016/j.envpol.2022.120359.

Guerrero, J.L., Gutiérrez-Álvarez, I., Hierro, A., Pérez-Moreno, S.M., Olías, M. & Bolívar, J.P. (2021a). Seasonal evolution of natural radionuclides in two rivers affected by acid mine drainage and phosphogypsum pollution. Catena 197, 104978. https://doi.org/10.1016/j.catena.2020.104978.

Guerrero, J.L., Pérez-Moreno, S.M., Gutiérrez-Álvarez, I., Gázquez, M.J. & Bolívar, J.P. (2021b). Behaviour of heavy metals and natural radionuclides in the mixing of phosphogypsum leachates with seawater. Environmental Pollution, 115843. https://doi.org/10.1016/j.envpol.2020.115843.

Guerrero, J.L., Gutiérrez-Álvarez, I., Mosqueda, F., Olías, M., García-Tenorio, R. & Bolívar, J.P. (2019). Pollution evaluation on the salt-marshes under the phosphogypsum stacks of Huelva due to deep leachates. Chemosphere 230, 219-229. https://doi.org/10.1016/j.chemosphere.2019.04.212.

Hakason, L. (1979). AN ECOLOGICAL RISK INDEX FOR AQUATIC POLLUTION CONTROL. A SEDIMENTOLOGICAL APPROACH. In Water Research (Vol. 14).

Hierro, A., Martín, J.E., Olías, M., García, C. & Bolívar, J.P. (2013). Uranium behavior during a tidal cycle in an estuarine system affected by acid mine drainage (AMD). Chemical Geology 342, 110-118.

Hierro, A., Bolívar, J.P., Vaca, F. & Borrego, J. (2012). Behavior of natural radionuclides in surficial sediments from an estuary impacted by acid mine discharge and industrial effluents in Southwest Spain Journal of Environmental Radioactivity 110, 13-23.

Kerolli-Mustafa, M., Fajković, H., Rončević, S., & Ćurković, L. (2015). Assessment of metal risks from different depths of jarosite tailing waste of Trepça Zinc Industry, Kosovo based on BCR procedure. Journal of Geochemical Exploration, 148, 161–168. https://doi.org/10.1016/j.gexplo.2014.09.001.

Lario, J., Alonso-Azcárate, J., Spencer, C., Zazo, C., Goy, J. L., Cabero, A., Dabrio, C. J., Borja, F., Borja, C., Civis, J., & García-Ródriguez, M. (2016). Evolution of the pollution in the Piedras River Natural Site (Gulf of Cadiz, southern Spain) during the Holocene. Environmental Earth Sciences, 75(6). https://doi.org/10.1007/s12665-016-5344-8.

Lee, P.-K., Lim, J., Jeong, Y.-J., Hwang, S., Lee, J.-Y., & Choi, B.-Y. (2021). Recent pollution and source identification of metal(loid)s in a sediment core from Gunsan Reservoir, South Korea. Journal of Hazardous Materials, 416, 126204. https://doi.org/10.1016/j.jhazmat.2021.126204.

Le Gall, M., Ayrault, S., Evrard, O., Laceby, J.P., Gateuille, D., Lefèvre, I., Mouchel, J.-M., & Meybeck, M. (2018). Investigating the metal contamination of sediment transported by the 2016 Seine River flood (Paris, France). Environmental Pollution, 240, 125-139. https://doi.org/10.1016/j.envpol.2018.04.082.

Liu, J., Deng, S., Liu, M., Liu, G., & Li, C. (2021). Distribution of heavy metals and radionuclides in the sediments and their environmental impacts in Nansha Sea area, South China Sea. Marine Pollution Bulletin, 166, 112192. https://doi.org/10.1016/j.marpolbul.2021.112192.

687 Luo, M., Kang, X., Liu, Q., Yu, H., Tao, Y., Wang, H., Niu, Y. & Niu, Y. (2022). Research on the
688 geochemical background values and evolution rules of lake sediments for heavy metals and nutrients in the
689 Eastern China Plain from 1937 to 2017. Journal of Hazardous Materials, 436, 129136.
690 https://doi.org/10.1016/j.jhazmat.2022.129136.

691 Morillo, J., Usero, J., & Gracia, I. (2004). Heavy metal distribution in marine sediments from the southwest
692 coast of Spain. Chemosphere, 55(3), 431–442. https://doi.org/10.1016/j.chemosphere.2003.10.047.

693 Mujica, B., Aurelio, J., & Macías, P. (2008). macla. nº 10. noviembre´08 revista de la sociedad española de
694 mineralogía.

695 Nieto, J.M., Sarmiento, A.M., Canovas, C.R., Olias, M. & Ayora, C. (2013). Acid mine drainage in the
696 Iberian Pyrite Belt: 1. Hydrochemical characteristics and pollutant load of the Tinto and Odiel rivers.
697 Environmental Science and Pollution Researh, 20 (11), 7509–7519. https://doi.org/10.1007/s11356-013-
698 1634-9.

699 Nieto, J.M., Sarmiento, A.M., Olías, M., Cánovas, C.R., Riba, I., Kalman, J. & Delvalls, T.A. (2007). Acid
700 mine drainage pollution in the Tinto and Odiel rivers (Iberian Pyrite Belt, SW Spain) and bioavailability of
701 the transported metals to the Huelva estuary. Environment International, 33, 445–455.
702 https://doi.org/10.1016/j. envint.2006.11.010.

703 Olías, M., Cánovas, C.R., Nieto, J.M. & Sarmiento, A.M. (2006). Evaluation of the dissolved contaminant
704 load transported by the Tinto and Odiel rivers (South West Spain). Applied Geochemistry, 21, 1733–1749.
705 https://doi.org/10.1016/j. apgeochem.2006.05.009.

706 Papaslioti, E. M., Pérez-López, R., Parviainen, A., Sarmiento, A. M., Nieto, J. M., Marchesi, C., Delgado-
707 Huertas, A., & Garrido, C. J. (2018). Effects of seawater mixing on the mobility of trace elements in acid
708 phosphogypsum leachates. Marine Pollution Bulletin, 127, 695–703.
709 https://doi.org/10.1016/j.marpolbul.2018.01.001.

710 Pérez-López, R., Macías, F., Cánovas, C. R., Sarmiento, A. M., & Pérez-Moreno, S. M. (2016). Pollutant
711 flows from a phosphogypsum disposal area to an estuarine environment: An insight from geochemical
712 signatures. Science of the Total Environment, 553, 42–51. https://doi.org/10.1016/j.scitotenv.2016.02.070.

713 Pérez-López, R., Nieto, J.M., López-Cascajosa, M.J., Díaz-Blanco, M.J., Sarmiento, A.M., Oliveira, V., &
714 Sánchez-Rodas, D. (2011). Evaluation of heavy metals and arsenic speciation discharged by the industrial
715 activity on the Tinto-Odiel estuary, SW Spain. Marine Pollution Bulletin, 62(2), 405–411.
716 https://doi.org/10.1016/j.marpolbul.2010.12.013.

717 Riba, I., Delvalls, T.A., Forja, J. M., & Gómez-Parra, A. (2002). Evaluating the heavy metal contamination
718 in sediments from the Guadalquivir estuary after the Aznalcóllar mining spill (SW Spain): A multivariate
719 analysis approach. Environmental Monitoring and Assessment, 77(2), 191–207.
720 https://doi.org/10.1023/A:1015828020313.

721 Royal Decree, 2005. Real Decreto 9/2005, de 14 de Enero, por el que se establece la relación de actividades
722 potencialmente contaminantes del suelo y los criterios y estándares para la declaración de suelos
723 contaminados.

724 Rudnick, R.L., & Gao, S. (2003). The Composition of the Continental Crust. In: Holland, H.D. and
725 Turekian, K.K., Eds., Treatise on Geochemistry, Vol. 3, The Crust, Elsevier-Pergamon, Oxford, 1-64.
726 http://dx.doi.org/10.1016/b0-08-043751-6/03016-4.

727 Sáez, R., Pascual, E., Toscano, M. & Almodóvar, G.R. (1999). The Iberian type of volcano–sedimentary
728 massive sulphide deposits. Mineralium Deposita, 34, 549–570. https://doi.org/10.1007/s001260050220.

729 Sousa, C. A. M., Delgado, J., Szalaj, D., & Boski, T. (2019). Holocene background concentrations and
730 actual enrichment factors of metals in sediments from Ria Formosa, Portugal. Marine Pollution Bulletin,
731 149. https://doi.org/10.1016/j.marpolbul.2019.110533.

732 UNSCEAR (2000). SOURCES AND EFFECTS OF IONIZING RADIATION United Nations Scientific
733 Committee on the Effects of Atomic Radiation UNSCEAR 2000 Report to the General Assembly, with
734 Scientific Annexes VOLUME I: SOURCES UNITED NATIONS.

735 Vineethkumar, V., Sayooj, V. V., Shimod, K. P., & Prakash, V. (2020). Estimation of pollution indices and
736 hazard evaluation from trace elements concentration in coastal sediments of Kerala, Southwest Coast of
737 India. Bulletin of the National Research Centre, 44(1). https://doi.org/10.1186/s42269-020-00455-0.

738 Yushin, N., Jakhu, R., Chaligava, O., Grozdov, D., & Zinicovscaia, I. (2023). Natural and anthropogenic
739 radionuclides concentration with heavy metals analysis of the sediments collected around Novaya Zemlya.
740 Marine Pollution Bulletin, 194, 2023. https://doi.org/10.1016/j.marpolbul.2023.115346.

741 Zhang, R., Guan, M., Shu, Y., Shen, L., Chen, X., Zhang, F., & Li, T. (2016). Historical record of lead
742 accumulation and source in the tidal flat of Haizhou Bay, Yellow Sea: Insights from lead isotopes. Marine
743 Pollution Bulletin, 106, 383-387. https://doi.org/10.1016/j.marpolbul.2016.02.046.